

String Tension versus Critical Temperature in Walking Regime

Albert Deuzeman^a, Maria Paola Lombardo^b, Kohtaroh Miura^{* b,c}, Tiago Nunes da Silva^d, Elisabetta Pallante^d

^a *Albert Einstein Center for Fundamental Physics, University of Bern, CH-3012 Bern, Switzerland*

^b *Laboratori Nazionali di Frascati, I-00044 Frascati (Rome), Italy*

^c *Kobayashi-Maskawa Institute for the Origin of Particles and the Universe, Nagoya University, Nagoya 464-8602, Japan*

^d *Centre for Theoretical Physics, University of Groningen, 9747 AG, Netherlands*

E-mail: miura@kmi.nagoya-u.ac.jp

We investigate the chiral phase transition temperature (T_c) in the unit of the string tension ($\sqrt{\sigma}$) for a various number of flavor (N_f) by using lattice Monte Carlo simulations. We show the first result on the ratio $T_c/\sqrt{\sigma}$ for $N_f = 6$ and 8, and compare it with those obtained for a smaller N_f . The ratio is found to be a decreasing function of N_f , and this indicates that the chiral dynamics becomes less significant in larger N_f region. We point out that our $T_c/\sqrt{\sigma}$ provides an important input for a model study on the many flavor QCD based on the gauge/gravity duality. Furthermore, we discuss the order of the chiral phase transition for $N_f = 8$.

31st International Symposium on Lattice Field Theory - LATTICE 2013

July 29 - August 3, 2013

Mainz, Germany

*Speaker.

1. Introduction

Novel conformal phase associated with the infra-red fixed point (IRFP) is anticipated to emerge in strongly-interacting non-Abelian gauge theories with the asymptotic freedom when the number of fermion species (N_f) exceeds a critical value ($N_f = N_f^*$) [1]. The quasi-conformal dynamics has been advocated as a basis for the dynamical symmetry breaking in the electroweak theory, which is referred as the walking technicolor model [2]. Lattice Monte-Carlo simulations are now expected to provide a solid theoretical base for this new class of the gauge theories [3].

The model studies based on the functional renormalization group [4] and the finite-temperature holographic gauge theory [5] indicate that the onset of the conformal window coincides with the vanishing of the chiral phase transition temperature (T_c), and the conformal phase appears as a zero-temperature limit of a possibly strongly-interacting quark gluon plasma (QGP). It is argued that the approach to the conformal phase shows a singular N_f dependence of T_c [4, 6] which may be regarded as a signal of the quasi-conformality.

The analysis of the finite-temperature chiral phase transition is a well-established line of research in the lattice QCD, and may allows us to evaluated the N_f^* from the vanishing of T_c based on the first-principle calculations. A quantity whose N_f dependences can be defined is to be dimensionless, and thus T_c should be normalized by some reference scale. The reference is then required to be insensitive to the physics of the chiral phase transition and the IRFP, otherwise the vanishing nature of T_c with increasing N_f is contaminated by the reference scale itself and gets invisible.

Recently, we have defined the normalized critical temperature (\hat{T}_c) by utilizing the two-loop beta-function, and estimated the onset of the conformal phase $N_f^* \sim 9.4 - 14.2$ via the vanishing of $\hat{T}_c(N_f)$ [7]. As a next step, it is preferable to define $\hat{T}_c(N_f)$ without recourse to the perturbative method. A simple example of the $\hat{T}_c(N_f)$ is the ratio between the transition temperature and the square-root of the string tension ($T_c/\sqrt{\sigma}$), which we investigate in this proceedings. We particularly investigate $T_c/\sqrt{\sigma}$ for $N_f = 6$ and 8, where the walking dynamics is suggested [3, 8, 9].

2. Simulation's Setup

We investigate $T_c/\sqrt{\sigma}$ for a single bare fermion mass $ma = 0.02$ by using the lattice Monte Carlo simulations. To this end, we utilize our recent results [7, 10] on the critical lattice coupling β_L^c associated with the chiral phase transition for $N_f = 6$ and 8:

$$\beta_L^c = \begin{cases} 5.025 & (N_f, N_t) = (6, 6) , \\ 4.275 & (N_f, N_t) = (8, 8) . \end{cases} \quad (2.1)$$

As shown in Ref. [7, 11, 10], the critical couplings have a thermal scaling, and are responsible for the physically-relevant thermal transition rather than the bulk transition. By using them as inputs for the zero temperature simulations with the lattice box size $32^3 \times 64$, we measure Wilson loops $W_{r,t}$ where the $r(t)$ denotes a spatial (temporal) extension. From the $W_{r,t}$, we evaluate the heavy-fermion potential $V(r)$, the effective mass m_{eff} , and the Creutz ratio $\chi_{r,t}$,

$$W_{r,t} = C(r)e^{-tV(r)} , \quad m_{\text{eff}}(r,t) = \log \left[\frac{W_{r,t}}{W_{r,t+1}} \right] = V(r) , \quad \chi_{r,t} = -\log \left[\frac{W_{r,t}W_{r+1,t+1}}{W_{r,t+1}W_{r+1,t}} \right] , \quad (2.2)$$

By fitting the lattice data with the ansatz

$$V(r) = V_0 - \frac{\alpha}{r} + \sigma r, \quad \text{or equivalently,} \quad \chi_{r,t} = \frac{\alpha}{\hat{r}(\hat{r}+1)} + \hat{\sigma}, \quad (2.3)$$

where $\hat{\sigma} = \sigma a^2$ and $\hat{r} = r/a$, we determine the normalized string tension $\hat{\sigma}$. We then investigate the dimensionless ratio $T_c/\sqrt{\sigma}$ as

$$\frac{T_c}{\sqrt{\sigma}} = \frac{T_c \cdot a(\beta_L^c)}{\sqrt{\sigma \cdot a^2(\beta_L^c)}} = \frac{N_t^{-1}}{\sqrt{\hat{\sigma}}}. \quad (2.4)$$

The left-hand side does not depend on N_t up to the scaling violation.

In the simulations for the Wilson loop measurements, we have used an improved version of the staggered action, the Asqtad action, with a one-loop Symanzik and tadpole improved gauge action. To generate configurations with mass degenerate dynamical flavours, we have used the rational hybrid Monte Carlo algorithm.

3. Results and Discussions

3.1 String Tension for $N_f = 6$ and 8

In Fig. 1, we show the Creutz ratio χ for $N_f = 6$ and 8 as a function of the spatial extension ra . The Creutz ratio can depend on the temporal extension, and we have determined it by taking the value of the plateau. The symbol + (red) at $ra = 1$ represents the results without a smearing, and the symbols “×” (blue) are the results with an Ape and a time-link smearing. The smearing parameters are adjusted to maximize the overlap function $C(r)$ appeared in the heavy-fermion potential (2.2). Although the smearing may affect the constant term V_0 as well as $C(r)$ of the heavy-fermion potential, the Creutz ratio does not depend on V_0 nor $C(r)$. Therefore, the comparison of the smeared and the non-smeared makes sense, and allows us to exclude the smearing artifacts: Apparently, the smeared result at $ra = 1$ is inconsistent to the non-smeared and should be excluded from the fit. The dashed line is the fit with the ansatz (2.3) for the smeared results in the region $[2, 7]$, and found to be consistent to the non-smeared result at $ra = 1$. This indicates that the smearing artifact becomes minor in $[2, 7]$. Combining this with the fact that the string tension σ is responsible for the large distance dynamics, the fit would be qualitatively reliable, and we find,

$$(\alpha, \sigma a^2) = \begin{cases} (0.551(18), 0.196(4)) & N_f = 6, \\ (0.479(35), 0.130(7)) & N_f = 8, \end{cases} \quad (3.1)$$

In order to evaluate σa^2 more quantitatively, we utilize the heavy-fermion potential, which is shown in Fig. 2. The data points represent the smeared results. To be consistent to the analyses of the Creutz ratio, we have excluded the data at $ra = 1$ from the fit (blue dashed line) and found,

$$(V_0, \alpha, \sigma a^2) = \begin{cases} (0.359(42), 0.640(58), 0.185(8)) & N_f = 6, \\ (0.447(65), 0.657(88), 0.117(12)) & N_f = 8, \end{cases} \quad (3.2)$$

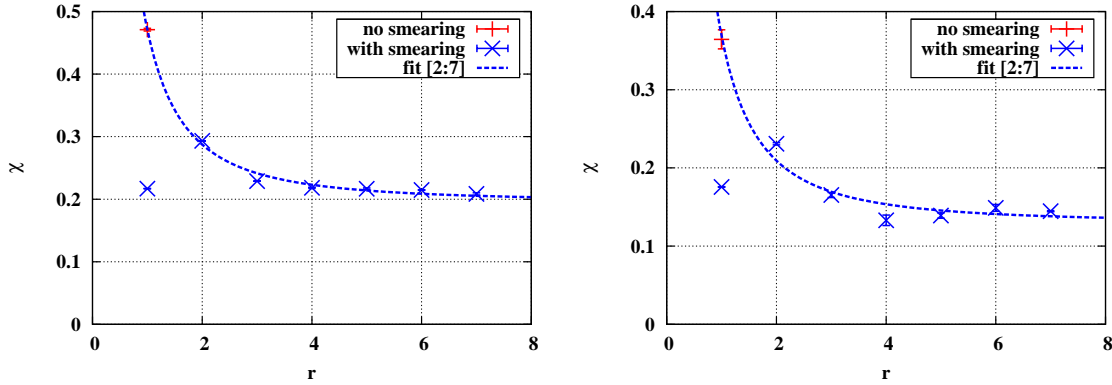


Figure 1: The Creutz ratio for $N_f = 6$ (left) and $N_f = 8$ (right). The symbol “+” (red) at $ra = 1$ represents the results without a smearing, and the symbols “x” (blue) are the results with a Ape and a time-link smearing. The dashed line is the fit for the smeared results in the region $[2, 7]$, and consistent to the non-smearred result at $ra = 1$.

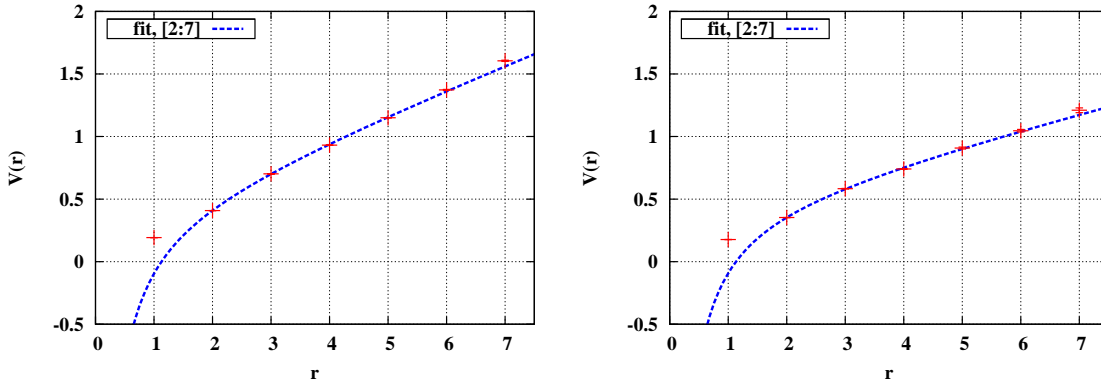


Figure 2: The heavy-fermion potential for $N_f = 6$ (left) and $N_f = 8$ (right) with an Ape and a time-link smearing. The dashed line is the fit for the data points in the region $[2, 7]$.

The difference between Eq. (3.1) and (3.2) would be regarded as a systematic error. We take the average of Eq. (3.1) and (3.2) and determine the error to include the maximum deviation from the average,

$$\sigma a^2 = \begin{cases} 0.191(14) & N_f = 6, \\ 0.124(19) & N_f = 8. \end{cases} \quad (3.3)$$

3.2 String Tension versus Critical Temperature

We evaluate the ratio $T_c/\sqrt{\sigma}$ by substituting the σa^2 obtained in previous subsection into (2.4), and compare the results with those for $N_f = 0 - 4$ [14, 15, 16]. Since the ratio has been obtained via the heavy-fermion potential fit for $N_f = 0 - 4$, we use the σa^2 shown in Eq. (3.2) rather than

(3.3), and we find,

$$\frac{T_c}{\sqrt{\sigma}} = \begin{cases} 0.388(8) & N_f = 6, \\ 0.365(17) & N_f = 8. \end{cases} \quad (3.4)$$

In Fig. 3, we show the ratio $T_c/\sqrt{\sigma}$ as a function of N_f . We see that the ratio is a decreasing function. This indicates that the chiral dynamics becomes less significant in larger N_f region. The decreasing trend becomes minor with increasing N_f , and does not seem to cross the N_f axis before the asymptotic freedom is lost ($N_f = 16.5$). This may not be surprising. We find at least two reasons for the non-vanishing $T_c/\sqrt{\sigma}$: First, the $\sqrt{\sigma}$ would not be a ‘‘UV’’ quantity and may also be vanishing when the conformal phase sets in. In other words, our result indicates that the regulator of T_c have to be more UV than $\sqrt{\sigma}$ to elucidate the vanishing of the chiral dynamics via the T_c . In this point of view, a quantity $T_c w_0$ where w_0 is a UV scale [17] defined by the Wilson flow [18] may be a candidate to be evaluated in future. Second, the finite bare fermion mass breaks the conformality, and both T_c and σ could be defined and finite even in the region $N_f \geq N_f^*$, where the N_f^* represents the lower edge of the conformal phase in the chiral limit. Thus bare fermion mass effects to $T_c/\sqrt{\sigma}(N_f)$ should be an important subject to be studied in future.

As indicated in Ref. [19], the ratio $T_c/\sqrt{\sigma}$ is one of the input parameters to set a scale in models based on the gauge/gravity duality at finite T . Such inputs for the (would-be) walking regime $N_f = 6$ and 8 are now available by the present study.

3.3 Discussion

The left panel of Fig. 4 shows ensemble averages of chiral condensates $a^3 \langle \bar{\psi} \psi \rangle$ (PBP) for $N_f = 8$ with the temporal extension $N_t = 8$. The blue (red) symbols represent the cold- (hot-) start results, which show the hysteresis at $\beta_L = 4.25$. The hysteresis indicates that the first-order transition exists around there: $\beta_L^c = 4.275$ [7]. Using the smaller temporal extension $N_t = 6$ in the same lattice setup [11], the first-order transition was observed at $\beta_L^c = 4.1125 \pm 0.0125$, which is smaller than the present result $\beta_L^c \sim 4.275$. The shift of β_L^c for a different N_t indicates that the hysteresis does not result from the bulk transition but from a physical thermal transition. This would be a potential interest in the electroweak baryogenesis scenario. We note that the mean-field based analysis for the anomaly [13] may not be robust in the walking regime due to the IRFP associated singularity [4, 6], and thus the observation of the first-order-like transition in the $N_f = 8$ is a non-trivial finding.

However, there is a caveat for this result. The right panel of Fig. 4 shows the effective mass of the Wilson loop measured with the smearing at zero temperature by using $\beta_L^c = 4.275$ as an

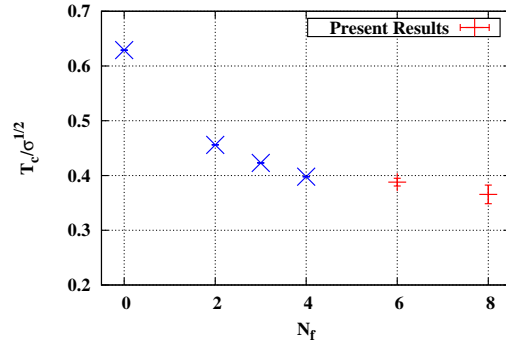


Figure 3: The $T_c/\sqrt{\sigma}$ as a function of N_f . The symbol + (red) represents the present results ($N_f = 6, 8$). For a comparison, we have quoted the $T_c/\sqrt{\sigma}$ from [14] ($N_f = 0$), [15] ($N_f = 2, 3$), [16] ($N_f = 4$).

input. We see the small oscillatory behavior. We have checked that the oscillation disappears in the non-smearing measurement. Such a lattice artifact indicates that the $\beta_L^c = 4.275$ or smaller corresponds to the strong coupling region. The observed hysteresis in the left panel may involve the sizable discretization error. In particular, the oscillation is reminiscent of the S_4 breaking phase [20] or the intermediate phase appearing between two bulk transitions in $N_f = 12$ QCD [21]. We should further investigate the transition property for $N_f = 8$ by using larger volume (N_t) to determine the critical lattice coupling β_L^c in the weaker coupling region, before concluding the emergence of the first-order thermal transition for $N_f = 8$.

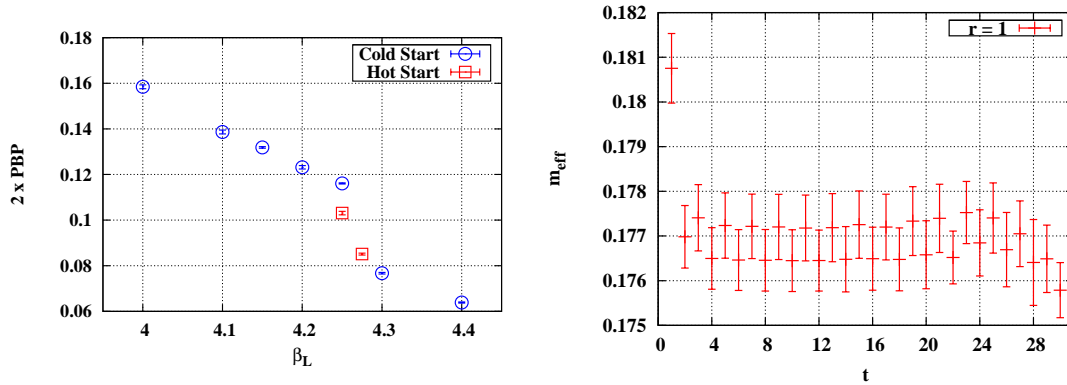


Figure 4: Left: The chiral condensate as a function of the lattice coupling β_L for $N_f = 8$. The lattice volume is $24^3 \times 8$ and the bare fermion mass is fixed to $ma = 0.02$. Right: The ta dependence of the effective mass of the Wilson loop at $ra = 1$. The small oscillation is visible.

4. Summary

We have investigated the chiral phase transition temperature (T_c) in the unit of the string tension ($\sqrt{\sigma}$) for a various number of flavor (N_f) by using Monte Carlo simulations. We have provided the first result on the ratio $T_c/\sqrt{\sigma}$ for $N_f = 6$ and 8. The ratio is found to be a decreasing function of N_f , which indicates that the chiral dynamics becomes less significant in larger N_f region. We have pointed out that the ratio $T_c/\sqrt{\sigma}$ for $N_f = 6, 8$ can be used in the Gauge/Gravity duality models. We have discussed a possibility of the first-order chiral transition for $N_f = 8$ based on the thermal scaling of the critical coupling. In fact, two critical couplings associated with the first-order-like chiral transition have shown the thermal scaling, which indicates the transition has a physical relevance. However, we have found a small oscillatory behavior results from the smearing in the effective mass of the Wilson loop measured at the critical coupling. This indicates that the first-order-like transition has been observed in the strong coupling region. In order to confirm the existence of the physical first-order transition, we need a simulation with a larger temporal extension (thereby the larger lattice volume) and a smaller lattice bare fermion mass. This should be considered as a future work.

Acknowledgements

We thank Marc Wagner for providing us the code for the Wilson loop measurement. This work was in part based on the MILC Collaboration's public lattice gauge theory code [22]. The numerical calculations for the chiral phase transition BG/P at CINECA in Italy and the Hitachi SR-16000 at YITP, Kyoto University in Japan. The numerical calculations for making the gauge configurations at zero temperature were performed in BG/Q at CINECA in Italy. The Wilson loop measurements were carried out on the high-performance computing system ϕ at KMI, Nagoya University in Japan.

References

- [1] W. E. Caswell, *Phys. Rev. Lett.* **33**, (1974) 244; T. Banks and A. Zaks, *Nucl. Phys. B* **196**, (1982) 189.
- [2] K. Yamawaki, M. Bando and K. -i. Matumoto, *Phys. Rev. Lett.* **56** (1986) 1335.
- [3] For recent reviews, see J. Kuti, to appear in PoS **LATTICE2013** (2013); E. Itou, to appear in PoS **LATTICE2013** (2013); J. Giedt, PoS **LATTICE2012** (2012) 006.
- [4] J. Braun, C. S. Fisher, and H. Gies, *Phys. Rev. D* **84** (2011) 034045; J. Braun and H. Gies, *JHEP* **1005** (2010) 060; **0606** (2006) 024.
- [5] T. Alho, M. Jarvinen, K. Kajantie, E. Kiritsis, and K. Tuominen, *JHEP* **1301**, (2013) 093.
- [6] V. A. Miransky and K. Yamawaki, *Phys. Rev. D* **55** (1997) 5051 [Erratum-ibid. *D* **56** (1997) 3768].
- [7] K. Miura and M. P. Lombardo, *Nuclear Physics B* **871** (2013), pp. 52 - 81.
- [8] T. Appelquist *et al.*, *Phys. Rev. Lett.* **104** (2010) 071601.
- [9] Y. Aoki, T. Aoyama, M. Kurachi, T. Maskawa, K. -i. Nagai, H. Ohki, A. Shibata and K. Yamawaki *et al.*, *Phys. Rev. D* **87** (2013) 094511; Y. Aoki, T. Aoyama, M. Kurachi, T. Maskawa, K. Miura, K. -i. Nagai, H. Ohki and E. Rinaldi *et al.*, arXiv:1309.0711 [hep-lat].
- [10] K. Miura, M. P. Lombardo and E. Pallante, *Phys. Lett. B* **710** (2012) 676.
- [11] A. Deuzeman, M. P. Lombardo and E. Pallante, *Phys. Lett. B* **670** (2008) 41.
- [12] A. Deuzeman, M. P. Lombardo and E. Pallante, *Phys. Rev. D* **82** (2010) 074503.
- [13] R. D. Pisarski and F. Wilczek, *Phys. Rev. D* **29** (1984), 338.
- [14] E. Laermann, *Nucl. Phys. A* **610** (1996) 1C.
- [15] F. Karsch, E. Laermann and A. Peikert, *Nucl. Phys. B* **605** (2001) 579.
- [16] J. Engels, R. Joswig, F. Karsch, E. Laermann, M. Lutgemeier and B. Petersson, *Phys. Lett. B* **396** (1997) 210.
- [17] S. Borsanyi, S. Durr, Z. Fodor, C. Hoelbling, S. D. Katz, S. Krieg, T. Kurth and L. Lellouch *et al.*, *JHEP* **1209** (2012) 010.
- [18] M. Luscher, *Commun. Math. Phys.* **293** (2010) 899.
- [19] U. Gursoy, E. Kiritsis, L. Mazzanti, G. Michalogiorgakis, and F. Nitti, *Lect. Notes Phys.* **828**, (2011) 79.
- [20] A. Cheng, A. Hasenfratz and D. Schaich, *Phys. Rev. D* **85** (2012) 094509.
- [21] A. Deuzeman, M. P. Lombardo, T. Nunes Da Silva and E. Pallante, *Phys. Lett. B* **720** (2013) 358.
- [22] MILC Collaboration, <http://www.physics.indiana.edu/~sg/milc.html>